Halogen Bonded Analogues of Deep Cavity Cavitands∗∗

N. Kodiah Beyeh,[a] Mario Cetina*[a,b] and Kari Rissanen*[a]*

[a] Department of Chemistry, NanoScience Center, University of Jyvaskyla, P. O. Box 35, 40014 Jyvaskyla, Finland
[b] Present address: Department of Applied Chemistry, Faculty of Textile Technology, University of Zagreb, Prilaz baruna Filipovića 28a, 10000, Zagreb, Croatia

Electronic Supplementary Information

Table of Contents

I General Information

The *N*-alkylammonium resorcinarene salts, **1-6**, were synthesized according to reported procedures.[1] CCl_3Br (**7**), 1,4-dioxane (**8**) and 1-butanol (**9**) were commercially available.^{1}H and ^{13}C NMR spectra were recorded on a Bruker Avance DRX 500 (500 MHz for ^{1}H and 126 MHz for ^{13}C) and a Bruker Avance DRX 400 (400 MHz for ^{1}H and 100 MHz for ^{13}C) spectrometers. All signals are given as δ values in ppm using residual solvent signals as the internal standard. Coupling constants are given in Hz. Melting points were determined with a Mettler Toledo FP62 capillary melting point apparatus. The mass spectrometric studies were performed with a micromass LCT ESI-TOF instrument equipped with a Z geometry electrospray ion source and a QSTAR Elite ESI-Q-TOF mass spectrometer equipped with an API 200 TurboIonSpray ESI source from AB Sciex (former MDS Sciex) in Concord, Ontario (Canada). All experiments were performed on positive polarization. The parameters of the ion source, ion optics and quadrupole were optimized to get maximum abundance of the ions under study.

II Synthesis

General Procedure for the synthesis of the of *N*-alkyl Ammonium Resorcinarene Chlorides:

a) Into a solution of resorcinarene (2 mmols) in ethanol (50 ml) and excess formaldehyde (5 ml), the amine (10 mmols) was added drop wise. The mixture was stirred at room temperature for 24 h. The precipitated product was filtered off, washed with cold ethanol/water (9:1 v/v) and dried to give the tetrabenzoxazine; b) Into a solution of the tetrabenzoxazine (0.5 mmols) in n-butanol (15 ml), conc. HCl (5 ml) and H_2O (5 ml) were added. The mixture was refluxed for 4 h. After the water and formaldehyde were removed by azeotropic distillation with chloroform, the remaining n-butanol was evaporated. The crude product was triturated with diethyl ether, filtered off and dried to give the *N*-alkylammonium resorcinarene chloride salt.

Synthetic details of *N*-cyclohexyl Ammonium Resorcinarene Chloride 4.

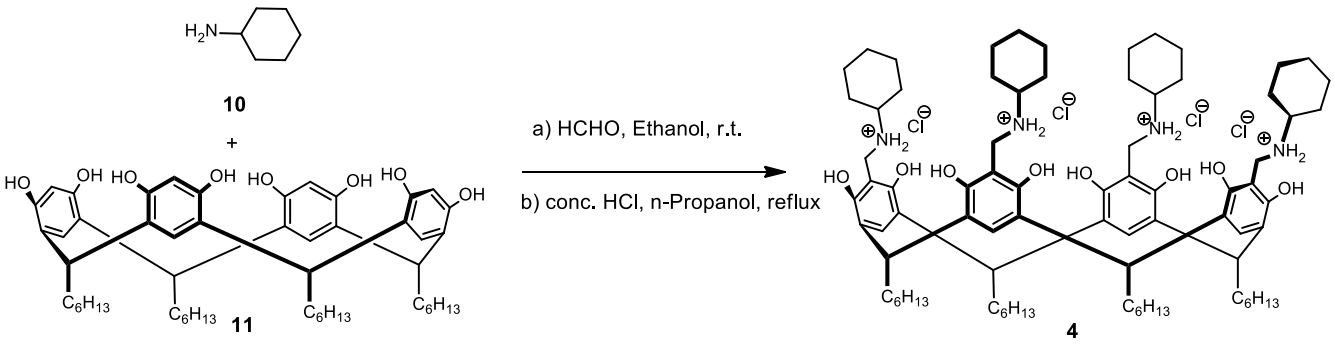

Scheme S1. Synthesis of *N*-cyclohexylammonium Resorcinarene Chloride **4**.

a) Resorcinarene **11** (4.1 g, 5.0 mmol), ethanol (50 ml), formaldehyde (5 ml), Cyclohexylamine **10** (2.5 mL, 22 mmol), tetrabenzoxazine (5.64 g, 86 %); b) Tetrabenzoxazine (1.8 g, 1.4 mmol), 2-propanol (40

ml), conc. HCl (9 ml), H_2O (20 ml), *N*-cyclohexylammonium resorcinarene chloride salt **4** (1.55 g, 80 %). m.p. > 279 ^oC; ^1H NMR (500 MHz, 303K in $CDCl_3$) δ: 0.88 (t, 12H, CH_3), 1.28 (m, 12H, CH_3), 1.38 (m, 8H, CH_2), 1.64 (m , 8H, CH_2), 1.77 (m , 8H, CH_2), 1.86 (m , 8H, CH_2) 2.17 (m , 8H, CH_2), 2.27 (m , 8H,N- CH_2), 3.15 (m , 4H, N-CH) 4.20 (m, 8H,Ar-CH_2-N), 4.30 (t, J=7.84 Hz , 4H, CH), 7.18 (s , 4H, Ar-H), 7,49(br , 8H, NH_2), 9,42(br , 8H, OH) ppm; ^{13}C NMR: (100 MHz, 303K in $CDCl_3$,) δ = 14.0, 22.6, 24.7, 24.7, 27.9, 28.6, 29.3, 31.8, 32.8, 34.3, 40.5, 59.2, 108.6, 124.7, 126.2, 150.2; ESI-QTRAP_MS (Positive ion mode, sprayed from MeOH): m/z = Found 1269.9477 ([M+H-4(HCl)]$^+$); calc. 1269.9492. Found 1305.9286 ([M+H-3(HCl)]$^+$); calc. 1305.9259.

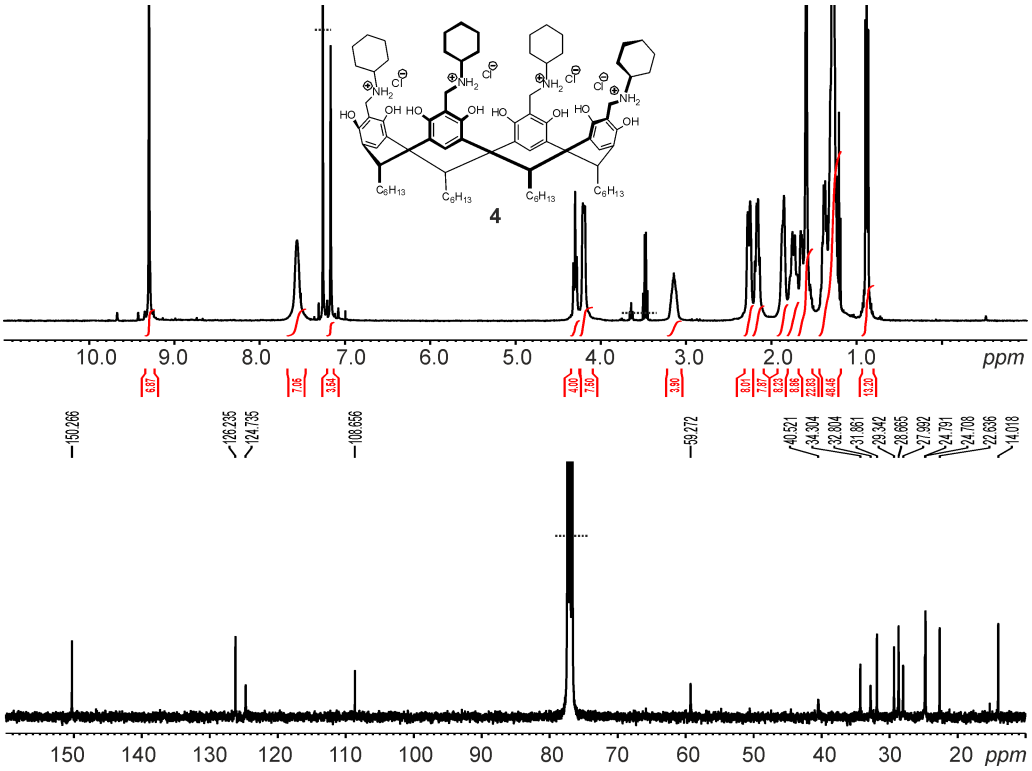

Fig. S1. ^1H and ^{13}C NMR spectra of *N*-cyclohexylammonium Resorcinarene Chloride **4**. The strikethrough lines represent solvent signals.

Synthetic details of *N*-benzyl Ammonium Resorcinarene Chloride 5.

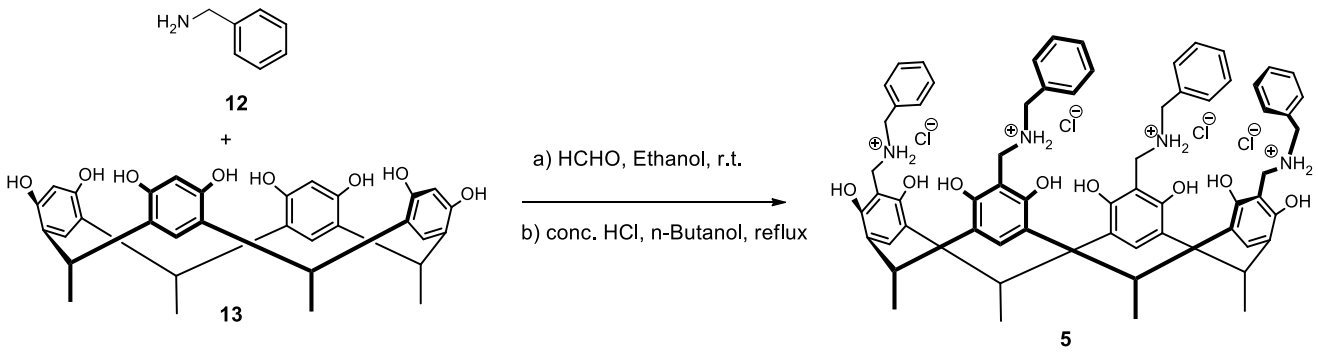

Scheme S2. Synthesis of resorcinarene salt **5**.

a) Resorcinarene **13** (1g, 1.84E-3 mols), ethanol (50 ml), formaldehyde (5 ml), benzylamine **12** (1.57 g, 0.015 mols), tetrabenzoxazine (1.96 g, 63 %); b) Tetrabenzoxazine (0.5 g, 4.67E-4 mols), n-butanol (15 ml), conc. HCl (5 ml), H_2O (5 ml), *N*-benzylammonium resorcinarene chloride salt **5** (0.3 g, 55 %).m.p. > 300 ^oC; ^1H NMR (400 MHz, 303K in $CDCl_3$) δ: 1.67 (d, J_{HH} = 7.23 Hz, 12H, CH_3), 4.04 (br, 8H, NCH_2Ar), 4.48 (q, J_{HH} = 7.15 Hz, 8H, CH), 7.23 (s, 4H, Ar-H), 7.41 (br, 8H, Ar-H), 7.67 (d, J_{HH} = 6.67 Hz, 8H, Ar-H), 8.20 (br, 4H, Ar-H), 8.95 (br, 8H, Ar-OH) ppm; ^{13}C NMR: (100 MHz, 303K in $CDCl_3$,) δ = 18.9, 28.6, 41.9, 51.9, 108.7, 124.3, 127.3, 129.0, 129.5, 129.6, 130.5, 149.9; ESI-TOF-MS (Positive ion mode, sprayed from CH_3CN/CH_2Cl_2 1:4 vv): m/z = 1021.5197 ($[M+H-2(HCl)]^+$); calc. 1021.5110.

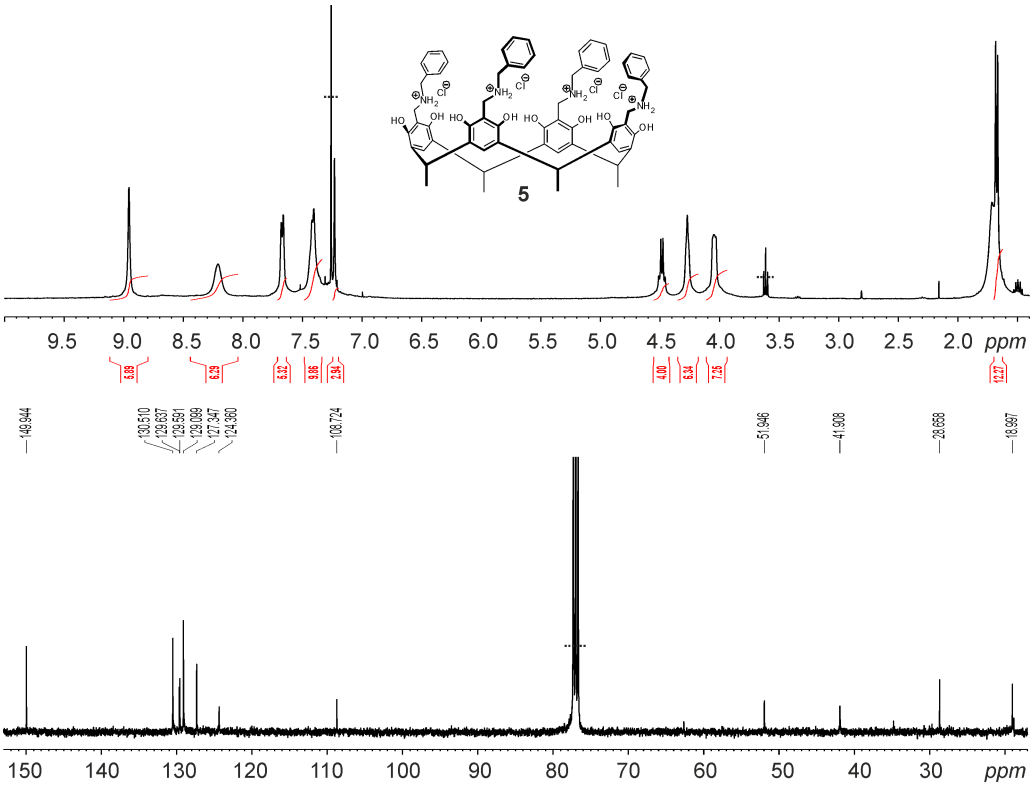

Fig. S2. ^1H and ^{13}C NMR spectra of *N*-benzylammonium Resorcinarene Chloride **5**.

III X-Ray Crystallogaphic Analysis

Structure of $\mathbf{1}(\mathbf{7})_4$

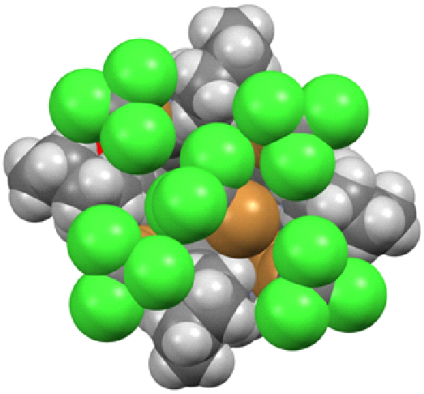

Fig. S3. CPK representation of $\mathbf{1}(\mathbf{7})_4$, showing position of the second CCl_3Br guest molecule which sits on top of the deep cavity included and badly disordered (occupancy 0.5) CCl_3Br in $\mathbf{1}(\mathbf{7})_4$.

Description of structures $\mathbf{5}(\mathbf{7})_{4.5}$ and $\mathbf{6}(\mathbf{7})_3$.

In the crystal structures of $\mathbf{5}(\mathbf{7})_{4.5}$ and $\mathbf{6}(\mathbf{7})_3$, the methylene groups between ammonium moieties and phenyl rings introduces flexibility to the resorcinarenes resulting in flower-like structures in which phenyl rings are oriented parallel to the plane of the hydrogen bond seam $(\cdots NR'R''H_2^+\cdots X^-\cdots NR'R''H_2^+\cdots X^-\cdots)_2$ (Figs S4 and S5). In these two halogen bonded complexes, compared to the analogue of a deep cavity cavitand $\mathbf{1}(\mathbf{7})_4$, the CCl_3Br molecules occupy completely different positions. In $\mathbf{5}(\mathbf{7})_{4.5}$ (Fig. S4), the four CCl_3Br molecules halogen bonded to the chloride anions are tilted approximately 45^o in respect to the plane of the hydrogen bond seam $(\cdots NR'R''H_2^+\cdots Cl^-\cdots NR'R''H_2^+\cdots Cl^-\cdots)_2$ while the fifth is located on the side of the resorcinarene tetracation with the C−Br bond being almost parallel to the plane of the ammonium cations and chloride anions.

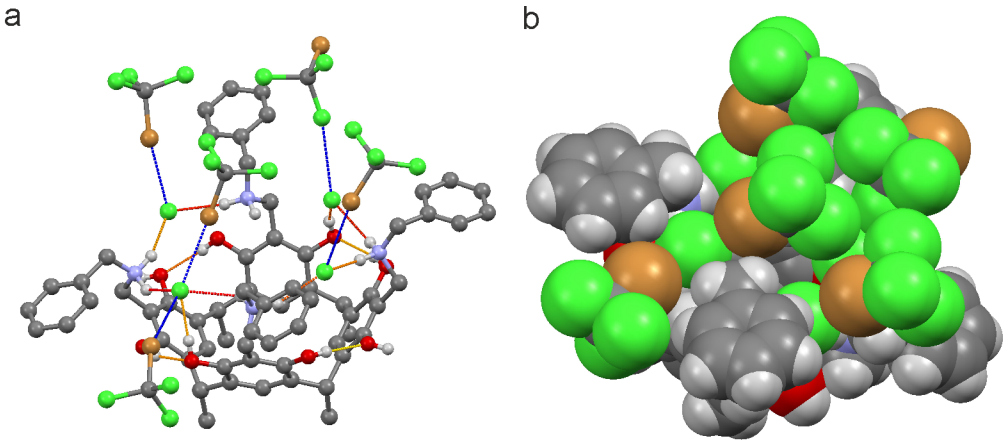

Fig. S4. Ball and stick representation of a side view (a) and CPK representation of a top view (b) of **5**(**7**)$_{4.5}$ showing halogen and hydrogen bond interactions and positions of CCl_3Br (**7**) molecules. In (a), hydrogen atoms that do not participate in intracomplex interactions are omitted for clarity.

Every resorcinarene cavity contains overall one water molecule and it is closed by CCl_3Br molecule which possess two different positions, and with C−Br bonds pointing to two different chlorides. Compared to the structure **1**(**7**)$_4$, the C−Br bond of one CCl_3Br molecule points to the chloride of a neighbouring resorcinarene salt. In every second salt molecule, one CCl_3Br molecule bonded to chloride and situated at the top of cavity is replaced with one water molecule. The R_{XB}^2 ranges from 0.90 to 0.94 indicating a slightly weaker XB than in **1**(**7**)$_4$. An additional interesting feature of this structure is that one of the chlorides participates in two halogen bonded interactions with two different CCl_3Br molecules.

Unlike the **1**(**7**)$_4$ and **5**(**7**)$_{4.5}$ the resorcinarene cation and the halogen bonded CCl_3Br molecule on top of the cation in **6**(**7**)$_3$ are situated on a symmetry element (2-fold axis) with Z' = 0.5. In the crystal structure of **6**(**7**)$_3$ (Fig. S5), three CCl_3Br molecules are halogen bonded to the bromides. Compared to previously described structures, two CCl_3Br molecules have completely different positions, with the C−Br bond being almost parallel to the phenyl ring plane, while one molecule which has two different orientations is placed at the top and closes the cavity.

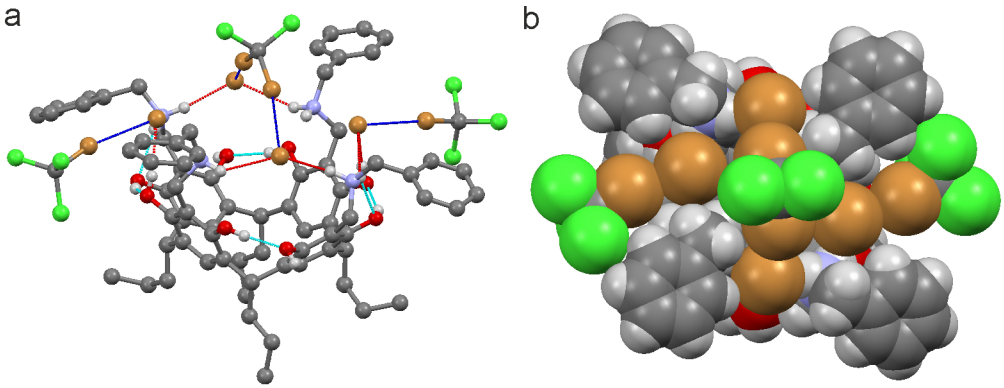

Fig. S5. Ball and stick representation of a side view (a) and CPK representation of a top view (b) of **6**(**7**)$_3$, showing halogen and hydrogen-bonding interactions and positions of CCl_3Br molecules. The CCl_3Br molecule at the top of the resorcinarene is presented in both orientations. In (a), hydrogen atoms that do not participate in intermolecular interactions are omitted for clarity.

The XB ratio[2] calculated for the two different XB's in **6**(**7**)$_3$ are 0.83 and 0.87, *i.e.* the CCl_3Br molecules are halogen bonded to the bromides slightly stronger than in the structure of **1**(**7**)$_4$. The conformation of the resorcinarene core in structures **5**(**7**)$_{4.5}$ and **6**(**7**)$_3$ is distorted. The distances between opposite nitrogens are 7.08 and 9.85 Å in **5**(**7**)$_{4.5}$, and 7.40 and 10.34 Å in **6**(**7**)$_3$.

X-ray crystallographic analysis of 1(7)$_4$, 8@4, 5(7)$_{4.5}$ and 6(7)$_3$

Data for **1**(**7**)$_4$ and **8**@**4** were collected at 123 K on a Bruker-Nonius Kappa Apex II diffractometer using graphite-monochromated MoK$_\alpha$ radiation (λ = 0.71073 Å). *COLLECT*[3] software was used for the data collection and *DENZO-SMN*[4] for the data processing. The intensities were corrected for absorption using the multi-scan absorption correction method. [5] For **5**(**7**)$_{4.5}$, and **6**(**7**)$_3$, data were collected at 123 K on an Agilent SuperNova Dual diffractometer with Atlas detector using mirror-monochromatized CuK$_\alpha$ radiation (λ = 1.54184 Å). The *CrysAlisPro*[6] program was used for the data collection and processing. The intensities were corrected for absorption using the analytical numeric absorption correction for **5**(**7**)$_{4.5}$ and multi-scan absorption correction for **6**(**7**)$_3$.[6] All four structures were solved by charge flipping with *SUPERFLIP*[7] and refined by full-matrix least-squares calculations based on F^2 using *SHELXL-2013*[8] integrated in the *WINGX*[9] program package. Hydrogen atoms were included in calculated positions as riding atoms, with *SHELXL-2013*[8] defaults.

The CCl_3Br molecules in **1**(**7**)$_4$ and **5**(**7**)$_{4.5}$ were heavily disordered and restraints on anisotropic thermal parameters and some geometric restraints were applied in their refinement. In **6**(**7**)$_3$, geometric restraints were applied in the refinement of CCl_3Br molecule designated as B. In **1**(**7**)$_4$, all chlorine atoms of CCl_3Br molecule A were disordered over two sites and were refined with fixed occupancy ratio of 80/20 %. Some constraints (EADP) were used in the refinement of these chlorine atoms and one bromine atom of G molecule. In **5**(**7**)$_{4.5}$, one chlorine and one bromine atom of CCl_3Br molecule A have two different positions and were refined with fixed occupancy ratio of 65/35 %. In the same structure, the CCl_3Br molecule D occupies two different positions and was refined with fixed occupancy ratio 50/50 %. The CCl_3Br molecule E and water oxygen atom were also refined with 50% occupancy.

Bromides Br1 to Br4 in **1**(**7**)$_4$ and chloride Cl1 in **5**(**7**)$_{4.5}$ were disordered over two sites and refined with fixed occupancy ratio of 75/25 % for bromides and 60/40 % for the chloride. Only five bromine atoms which represent five different orientation of heavily disordered CCl_3Br molecule were found in the Fourier map of **1**(**7**)$_4$ and were refined in such a way that sum of the occupancy for all 5 atoms amounts 0.75. Furthermore, restraints on anisotropic thermal parameters were applied in the refinement of disordered chloride Cl'1 and water oxygen O2W atom, as well as some constraints (EADP) in the refinement of carbon atom of chloroform molecule in **5**(**7**)$_{4.5}$. In **5**(**7**)$_{4.5}$, $CHCl_3$ molecule F occupy two different positions and were refined with fixed occupancy ratio 50/50 %. In **6**(**7**)$_3$, restraints on anisotropic thermal parameters were applied in the refinement of bromides Br1 and Br2.

Restraints on anisotropic thermal parameters and some geometric restraints were applied in the refinement of some carbon phenyl ring atoms in **5**(**7**)$_{4.5}$. Some geometric restraints and restraints on anisotropic thermal parameters were applied in the refinement of cyclohexyl rings and hexyl groups in **8**@**4**. Constraints on anisotropic thermal parameters (EADP) were also applied in the refinement of some hexyl ring atoms. The 1,4-dioxane molecule in **8**@**4** is disordered and is refined as two molecules with fixed occupancy ratio of 65/35%. Restraints on anisotropic thermal parameters and some geometric restraints were applied in the refinement. Structures of **1**(**7**)$_4$ and **5**(**7**)$_{4.5}$ contains small amount of crystal lattice water. Hydrogen atoms for water oxygens were not found in the Fourier map.

As a consequence of heavily disordered CCl_3Br molecules in **1**(**7**)$_4$ and **5**(**7**)$_{4.5}$ high residual electron densities were observed, 4.17 eÅ^{-3} for **1**(**7**)$_4$ [0.50 Å from disordered Cl3'] and 4.38 eÅ^{-3} for

5(**7**)$_{4.5}$ [1.13 Å from disordered Cl5F]. In **1**(**7**)$_4$, diffrn_measured_fraction_theta_full is 0.954 what resulted in checkCIF B level Alert. This is caused by the fact that crystal did not diffract at higher angles. The solvent accessible cavity void volume in **1**(**7**)$_4$ was calculated to be *ca.* 550 Å^3 [*SQUEEZE*[10] routine inside *PLATON*[11] after removal of the included CCl_3Br molecules]. Structures of **8**@**4** and **6**(**7**)$_3$ contain solvent accessible voids of *ca.* 383 and 84 A^3, respectively, with small amount of solvent molecule(s) used for recrystallization. As they could not be modeled satisfactorily data were treated with the *SQUEEZE*[10] routine in *PLATON*.[11]

The CCDC 967819-967822 contain the supplementary crystallographic data for this paper [**1**(**7**)$_4$, **8**@**4**, **5**(**7**)$_{4.5}$ and **6**(**7**)$_3$]. These data can be obtained free of charge from The Cambridge Crystallographic Data Centre *via* www.ccdc.cam.ac.uk/data_request/cif.

Crystal data for 1(7)$_4$:
$C_{69.50}H_{96}Br_{10.25}Cl_{16.50}N_4O_{10.50}$, M_r = 2559.5; 0.30 x 0.25 x 0.10 mm^3, monoclinic space group $P\ 2_1/n$ (No. 14); a = 17.7068(4), b = 31.1489(9), c = 18.8860(5) Å; β = 90.783(2)^o; V = 10415.5(5) Å^3; Z = 4; d_x = 1.632 g cm^{-3}; μ = 4.415 mm^{-1}; θ_{max} = 25.5^o; 18449 unique and 10680 reflections with $I \geq 2\sigma(I)$; R_{int} = 0.0755; 1097 parameters and 90 restraints; S = 1.178; $R[I \geq 2\sigma(I)]$ = 0.1163, *wR*[all data] = 0.3863; 4.171<Δρ<– 2.307 eA^{-3}.
Crystal data for 8@4:
$C_{84}H_{136}Cl_4N_4O_{10}$, M_r = 1503.76; 0.50 x 0.27 x 0.23 mm^3, triclinic space group P -1 (No. 2); a = 14.9721(4), b = 16.4049(5), c = 20.2775(5) Å; α = 77.8360(10), β = 83.606(2), γ = 63.8360(10)^o; V = 4368.8(2) Å^3; Z = 2; d_x = 1.143 g cm^{-3}; μ = 0.191 mm^{-1}; θ_{max} = 25.5^o; 16172 unique and 10486 reflections with $I \geq 2\sigma(I)$; R_{int} = 0.0471; 973 parameters and 111 restraints; S = 1.040; $R[I \geq 2\sigma(I)]$ = 0.1087, *wR*[all data] = 0.3413; 1.875<Δρ<– 1.074 eA^{-3}.
Crystal data for 5(7)$_{4.5}$:
$C_{69.50}H_{73}Br_{4.50}Cl_{20.50}N_4O_{9.50}$, M_r = 2202.63; 0.54 x 0.10 x 0.08 mm^3, triclinic space group $P\ \bar{1}$ (No. 2); a = 15.6587(6), b = 15.7044(6), c = 20.3684(6) Å; α = 92.294(3), β = 110.286(3), γ = 98.735(3)^o; V = 4620.4(3) Å^3; Z = 2; d_x = 1.583 g cm^{-3}; μ = 8.263 mm^{-1}; θ_{max} = 67.0^o; 16316 unique and 12955 reflections with $I \geq 2\sigma(I)$; R_{int} = 0.0344; 1119 parameters and 133 restraints; S = 1.814; $R[I \geq 2\sigma(I)]$ = 0.1389, *wR*[all data] = 0.4264; 4.379<Δρ<–3.345 eA^{-3}.
Crystal data for 6(7)$_3$:
$C_{75}H_{88}Br_7Cl_9N_4O_8$, M_r = 2051.91; 0.13 x 0.10 x 0.05 mm^3, monoclinic space group $C\ 2/c$ (No. 15); a = 29.3897(13), b = 13.9188(3), c = 27.2095(12) Å; β = 128.814(7)^o; V = 8672.8(9) Å^3; Z = 4; d_x = 1.571 g cm^{-3}; μ = 6.858 mm^{-1}; θ_{max} = 67.0^o; 7651 unique and 6898 reflections with $I \geq 2\sigma(I)$; R_{int} = 0.0215; 480 parameters and 14 restraints; S = 1.035; $R[I \geq 2\sigma(I)]$ = 0.0543, *wR*[all data] = 0.1579; 1.585<Δρ<– 2.035 eA^{-3}.

IV NMR Spectroscopic Analysis

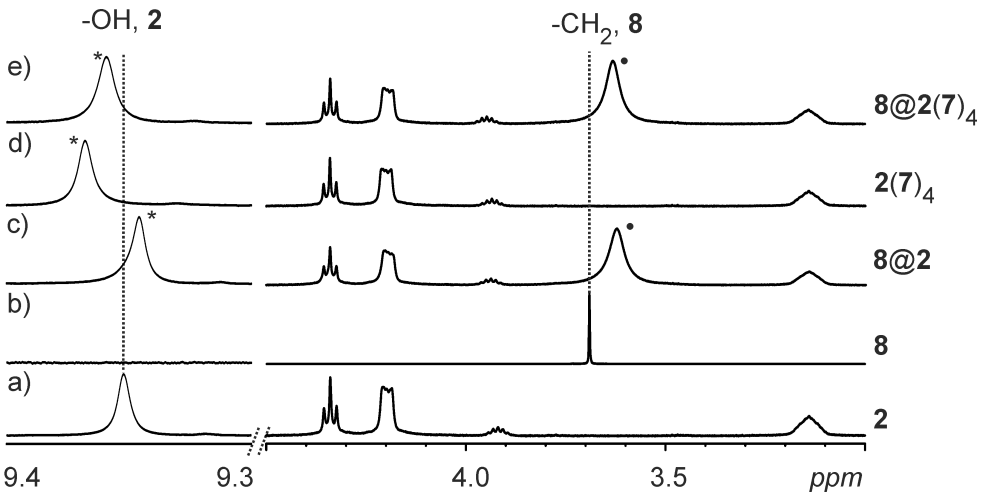

Fig. S6. Partial ^{1}H NMR spectra of several combinations of host **2**, XB donor **7** and guest **8**. * indicate the signal shifts of the hydroxyl groups of the host **2** and • indicate the signal shift of the guest **8**. Dotted lines are references of the position of the free host **2** and guest **8** and give an indication of the shift resulting from interaction between the compounds.

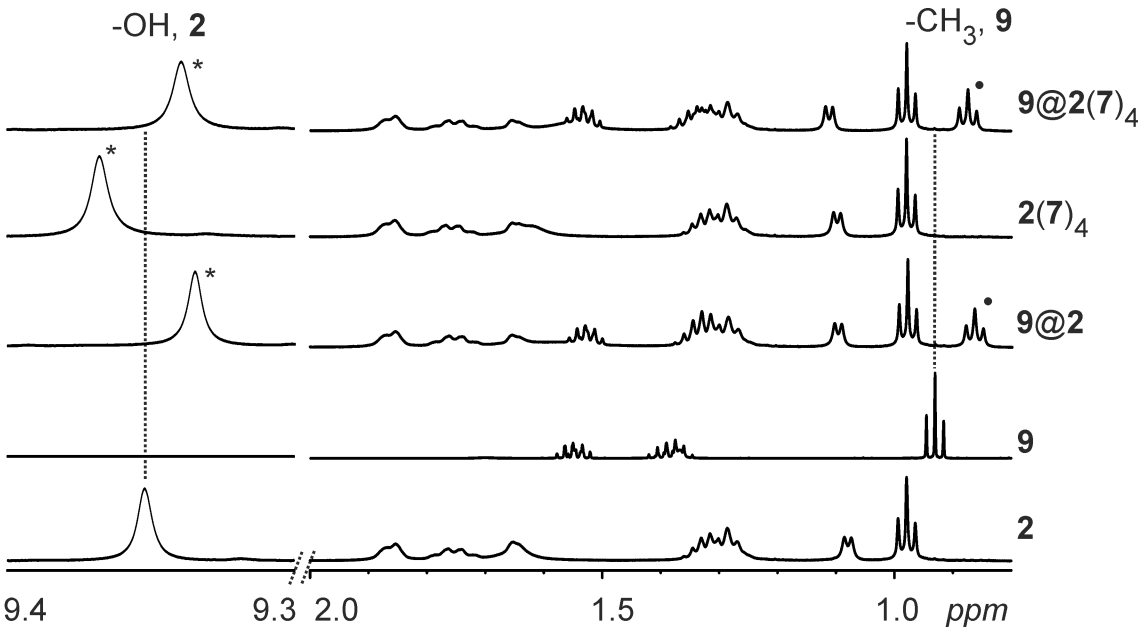

Fig. S7. Partial ^{1}H NMR spectra of several combinations of host **2**, XB donor **7** and guest **9**. * indicate the signal shifts of the hydroxyl groups of the host **2** and • indicate the signal shift of the guest **9**. Dotted lines are references of the position of the free host **2** and guest **9** and give an indication of the shift resulting from interaction between the compounds.

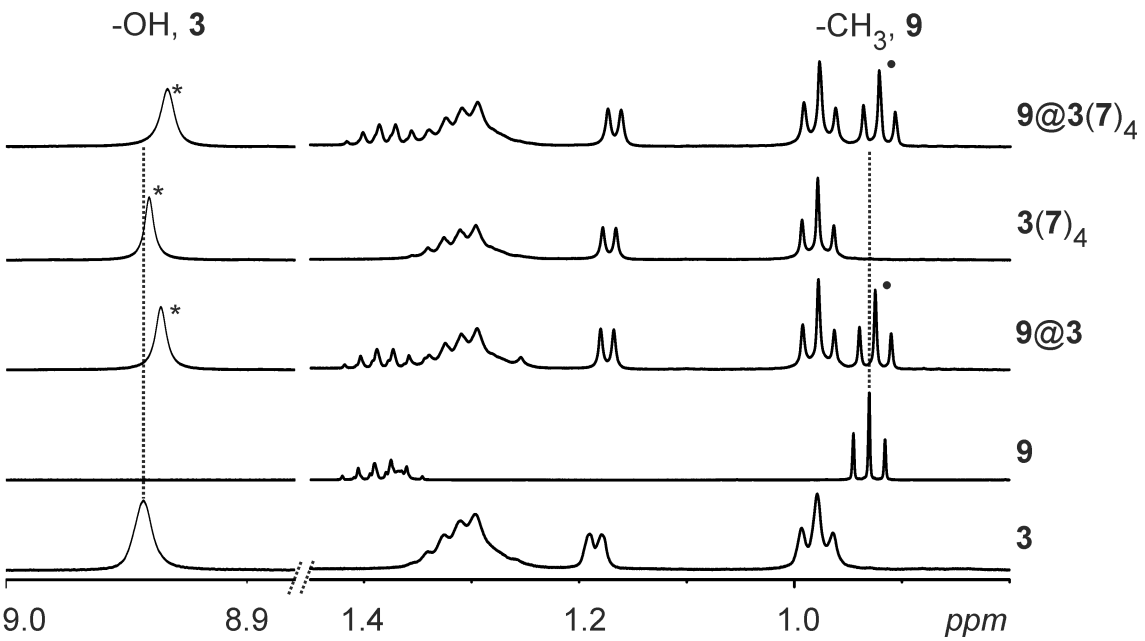

Fig. S8. Partial ^{1}H NMR spectra of several combinations of host **3**, XB donor **7** and guest **9**. * indicate the signal shifts of the hydroxyl groups of the host **3** and • indicate the signal shift of the guest **9**. Dotted lines are references of the position of the free host **3** and guest **9** and give an indication of the shift resulting from interaction between the compounds.

Table 1 ^{1}H NMR chemical shift difference of the different assemblies in Hz.[a]

Assemblies	-OH (**2**/**3**)	-NH_2 (**2**/**3**)	-CH_2 (**8**)	-CH_3 (**9**)
2(**7**)$_4$	+7.87	-7.14	-	-
8@**2**	-3.14	+8.52	-34.06	-
9@**2**	-8.75	+14.64	-	-33.41
8@**2**(**7**)$_4$	+3.58	+2.73	-29.67	-
9@**2**(**7**)$_4$	-6.30	+10.32	-	-
3(**7**)$_4$	-1.37	Overlap	-	-
8@**3**	-7.71	+10.32	-24.40	-
9@**3**	-5.01	+4.58	-	-4.49
8@**3**(**7**)$_4$	-6.08	+7.64	-19.90	-
9@**3**(**7**)$_4$	-3.59	+2.90	-	-2.90

[a] ^{1}H NMR in $CDCl_3$ at 303 K.

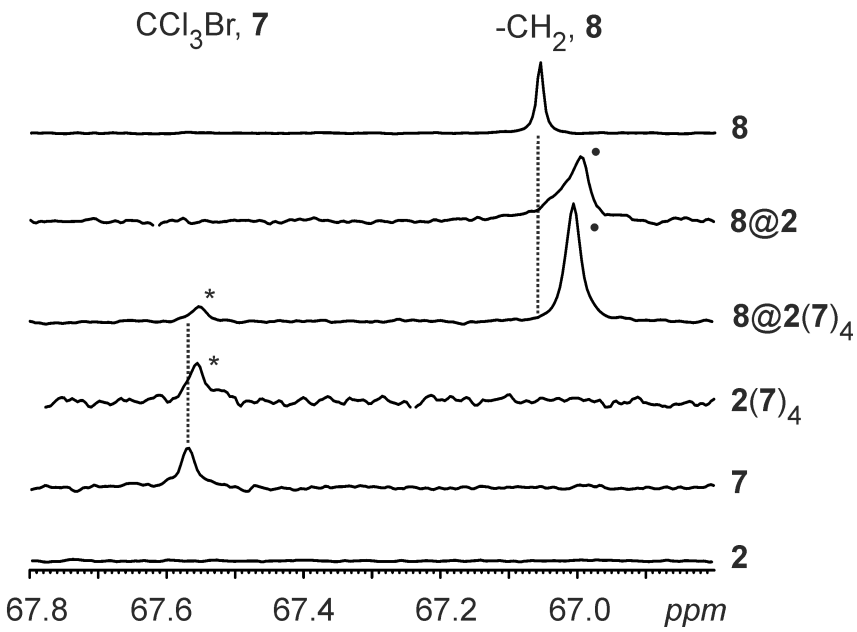

Fig. S9. Partial ^{13}C NMR spectra of several combinations of host **2**, XB donor **7** and guest **8**. * indicate the signal shifts of **7** carbon and • indicate the signal shifts of the –CH_2 carbon of the guest **8**. Dotted lines are references of the position of the free host **2** and guest **8** and give an indication of the shifts resulting from interaction between the compounds.

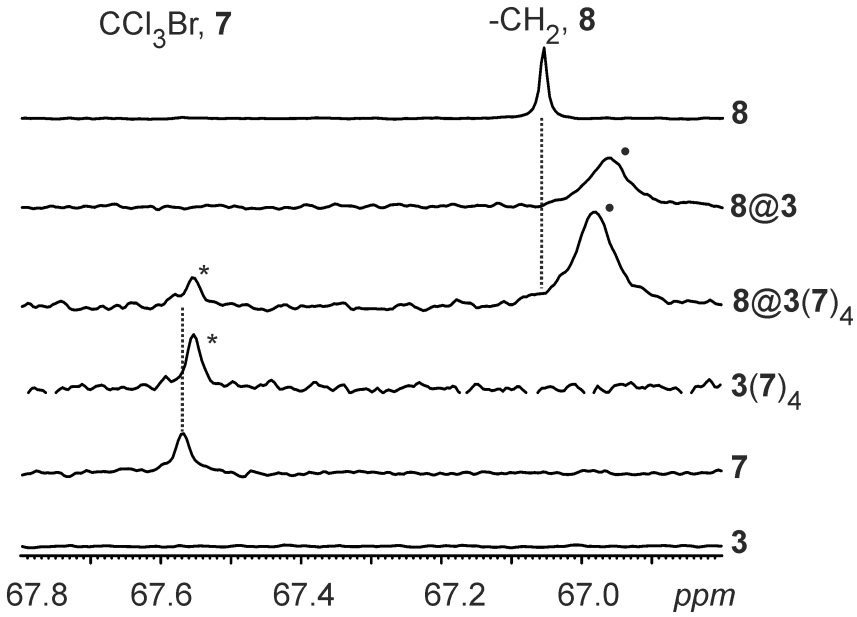

Fig. S10. Partial ^{13}C NMR spectra of several combinations of host **3**, XB donor **7** and guest **8**. * indicate the signal shifts of **7** carbon and • indicate the signal shifts of the –CH_2 carbon of the guest **8**. Dotted lines are references of the position of the free host **3** and guest **8** and give an indication of the shifts resulting from interaction between the compounds.

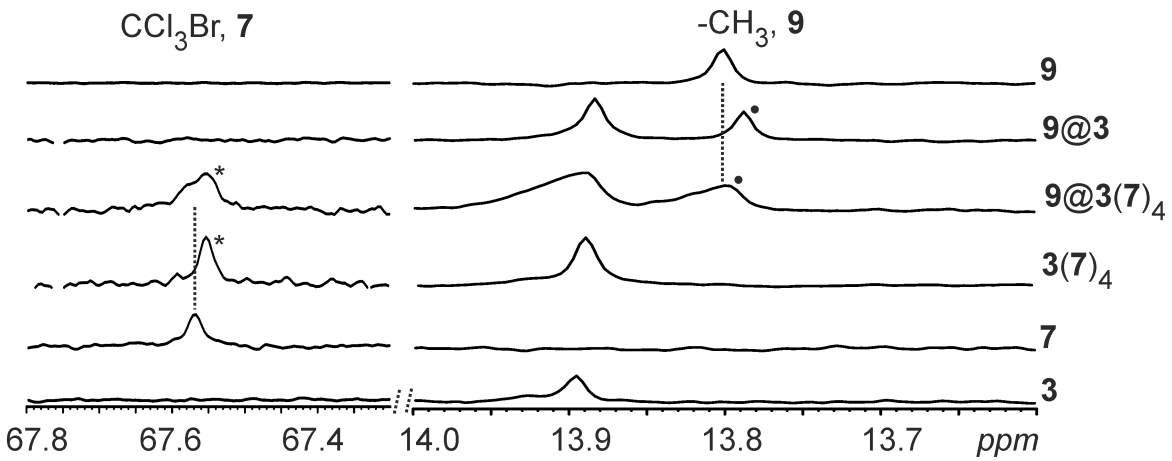

Fig. S11. Partial ^{13}C NMR spectra of several combinations of host **3**, XB donor **7** and guest **9** as guest. * indicate the signal shifts of **7** carbon and • indicate the signal shifts of the $–CH_3$ carbon of the guest **9**. Dotted lines are references of the position of the free host **3** and guest **9** and give an indication of the shifts resulting from interaction between the compounds.

Table 2 ^{13}C NMR chemical shift difference of the different assemblies in Hz. [a]

Assemblies	CCl_3Br (**7**)	$-CH_2$ (**8**)	$-OCH_2$ (**9**)	$-CH_3$ (**9**)
2(**7**)$_4$	-1.37	-	-	-
8@**2**	-	-5.95	-	-
9@**2**	-	-	-3.63	-9.86
8@**2**(**7**)$_4$	-i.60	-5.01	-	-
9@**2**(**7**)$_4$	-1.57	-	-2.67	-9.02
3(**7**)$_4$	-1.56	-	-	-
8@**3**	-	-9.35	-	-
9@**3**	-	-	+3.17	-1.29
8@**3**(**7**)$_4$	-1.57	-7.36	-	-
9@**3**(**7**)$_4$	-1.00	-	+5.99	+0.38

[a] ^{13}C NMR in $CDCl_3$ at 303 K

V References:

1 (a) A. Shivanyuk, T. Spaniol, K. Rissanen, E. Kolehmainen, V. Böhmer, *Angew. Chem., Int. Ed.* 2000, **39**, 3497-3500; (b) N. K. Beyeh, M. Cetina, K. Rissanen, *Cryst. Growth Des.* 2012, **12**, 4919-4926; (c) N. K. Beyeh, M. Cetina, M. Lofman, M. Luostarinen, A. Shivanyuk, K. Rissanen, *Supramol. Chem.* 2010, **22**, 737-750.

2 (a) P. M. Lommerse, A. J. Stone, R. Taylor and F. H. Allen, *J. Am. Chem. Soc.,* 1996, **118***,* 3108. (b) L. Brammer, E. A. Bruton and P. Sherwood, *Cryst. Growth Des*., 2001, **1**, 277. (c) F. Zordan, L. Brammer and P. Sherwood, *J. Am. Chem. Soc.* 2005, **127**, 5979. R_{XB} = r(X…D)/sum(X_{vdw} + D_{vdw}), where r(X…D) is the distance between the halogen bond donor (X) and halogen bond acceptor (D) in Å. X_{vdw} is the van der Waals radii of the halogen bond donor atom and D_{vdw} is the van der Waals radii of the halogen bond acceptor, both in Å. Thus R_{XB} is a plain number. $X_{vdw,Br}$ = 1.85 Å, D_{vdw} = Cl^- 1.81, Br^- 1.96 Å.

3 R. W. W. Hooft, *COLLECT*; Nonius BV, Delft, The Netherlands, 1998.

4 Z. Otwinowski and W. Minor, in *Methods in Enzymology* Vol. *276* (Eds.C. W. Carter Jr., R. M. Sweet), Academic Press, New York, 1997.

5 G. M. Sheldrick, *SADABS* 2008/2; University of Göttingen, Göttingen, Germany, 2008.

6 Oxford Diffraction, Xcalibur CCD System. *CRYSALISPRO*; Oxford Diffraction Ltd: Abingdon, England, 2013.

7 L. Palatinus, G. Chapuis, *J. Appl. Crystallogr.* 2007, **40**, 786-790.

8 G. M. Sheldrick, *Acta Crystallogr.* 2008, **A64**, 112-122.

9 L. J. Farrugia, *J. Appl. Crystallogr.* 1999, **32**, 837-838.

10 P. v.d. Sluis, A. L. Spek, *Acta Crystallogr.* 1990, **A46**, 194-201.

11 A. L. Spek, *J. Appl. Crystallogr.* 2003, **36**, 7-13.